Stimulated Raman scattering from individual single-wall carbon nanotubes

B. P. Zhang[a)]
Advanced Device Laboratory, RIKEN, 2-1 Hirosawa, Wako 351-0198, Japan and Semiconductor Photonics Research Centre, Department of Physics, Xiamen University, Xiamen 361005, P.R. China

K. Shimazaki
Graduate School of Science and Technology, Chiba University, Chiba 263-8522, Japan

T. Shiokawa, M. Suzuki, and K. Ishibashi
Advanced Device Laboratory, RIKEN, 2-1 Hirosawa, Wako 351-0198 and CREST, Japan Science and Technology Agency (JST), Kawaguchi 332-0012, Japan

R. Saito
Department of Physics, Tohoku University, Sendai and CREST, Japan Science and Technology Agency (JST), Kawaguchi 332-0012, Japan

(Received 12 December 2005; accepted 11 May 2006; published online 12 June 2006)

Individual single-wall carbon nanotubes (SWNTs) exhibited continuous-wave stimulated Raman scattering (SRS). The Raman gain is a few orders higher, and the threshold power is a few orders lower, than values ever reported for other bulk materials and is explained as the result of both the large nonlinear property and efficient electron-phonon interaction in the SWNT. The laser-induced variation of the peak position of the SRS line was likely to depend on the linewidth or tube quality. The results demonstrate the high potential of SWNTs in applications of nanoscale nonlinear optical devices such as wide-range tuneable Raman lasers. © *2006 American Institute of Physics*.
[DOI: 10.1063/1.2211054]

Semiconducting single-wall carbon nanotubes (SWNTs), which are characterized by direct band gaps, can emit light from the visible to the infrared spectral region and light emission by current injection has been demonstrated.[1,2] Large nonlinearity has also been found when the wavelength of the incident light wave is resonant with band-to-band transitions in the SWNTs.[3] We have fabricated luminescent SWNTs suspended on SiO_2 pillars, and strong photoluminescence at room temperature in the near infrared spectral region was observed.[4] In this letter, we report the stimulated Raman scattering (SRS) observed from such suspended SWNTs. The Raman gain was much larger than the values previously obtained from conventional semiconductors and the threshold power for SRS is substantially small.

Electron beam lithography and reactive ion etching (RIE) were employed to fabricate SiO_2 pillars on Si substrates.[4] The thicknesses of the SiO_2 film, which is equal to the height of the pillars, were 250–500 nm. Ni metal was used as a mask material for the RIE. The top surfaces of pillars are SiO_2, whereas other surfaces are Si on which no formation of SWNTs are expected due to the silicidation of the catalyst. SWNTs were synthesized at temperatures of 600–900 °C and under pressures of 0.05–1700 Pa with chemical vapor deposition (CVD). The growth time was 10–200 min. Co (0.1 nm thickness) and ethanol were used as the catalyst and carbon source, respectively. The morphology of the samples was examined using a scanning electron microscope (SEM). Figure 1 shows an example of SEM images of suspended SWNTs between SiO_2 pillars with a pillar distance of 1 μm. A micro Raman system was used to measure the Raman spectra of the SWNTs. A He–Ne laser (632.8 nm) was used as the excitation source and the laser spot was focused to ~1 μm in diameter. A backscattering configuration was adopted for Raman spectroscopy, where the propagating vector of both the incident laser and the scattered light is normal to the tube axis. The polarization of the electric vector of the incident laser was rotated to reach a maximum Raman intensity. In this case, the polarization is considered to be parallel to the tube axis. Then the laser power was varied smoothly in small steps by combination of filters having different transmittances. We would like to emphasize that this control of laser power is essential in order to observe SRS because, as shown below, the Raman intensity grows very quickly and easily saturates even at a low laser power. The room-temperature Raman signal was detected using a charge-coupled device. The accumulation time for each spectrum was varied from a few seconds to a few minutes, depending on the laser power and signal intensity. Thus in

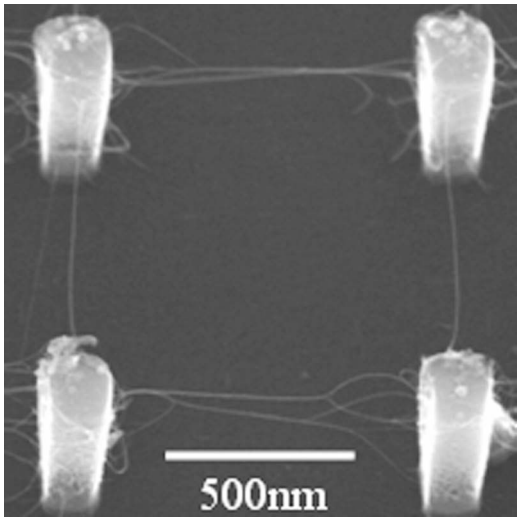

FIG. 1. SEM images of suspended SWNTs between SiO_2 pillars.

[a)]Electronic mail: bzhang@xmu.edu.cn

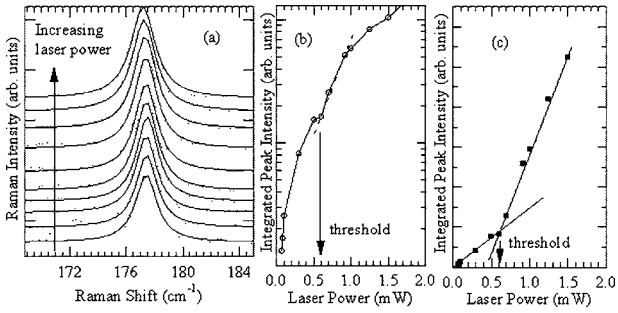

FIG. 2. (a) Raman spectra of a RBM mode at $\sim$177.5 cm^{-1} under different excitation laser intensities (from bottom: 0.07, 0.08, 0.1, 0.3, 0.5, 0.6, 0.7, 1.0, 1.25, and 1.5 mW). Each spectrum was normalized by the peak intensity and offset vertically for clarity. The dotted spectra are measured results and solid ones are Lorentzian fittings. [(b) and (c)] Plot of the integrated peak intensity as a function of laser intensity in logarithm-linear and linear-linear scales, respectively. The threshold of laser intensity for stimulated Raman scattering was 0.6 mW. The solid lines are guides for the eye. The dashed line shows the slope from which the Raman gain was obtained.

order to observe SRS threshold energy, it is essential to change the laser power around 0.1 mW and to take an accumulation time of about several minutes for each laser power.

From these suspended SWNTs, we observed clear Raman peaks in the radial breathing mode (RBM) region (100–400 cm^{-1}) and the splitting of the G band ($\sim$1600 cm^{-1}).[4] In general, the intensity of the Raman lines increases linearly with an increase in the laser power. In our experiments, however, Raman lines having narrow widths (basically $\leqslant$6 cm^{-1}) exhibited a sudden rise in their intensity at some threshold laser power, while those having broad widths (more than 6 cm^{-1}) show a linear response of the power. Figure 2 shows an example of the Raman spectra of the RBM peak with a narrow width and the integrated peak intensity as a function of laser power. The peak parameters were obtained by fitting each Raman spectrum using a single Lorentzian profile. The intensity-power plot was given in both logarithm-linear and linear-linear scales. The Raman peak frequency was $\sim$177.5 cm^{-1}, which does not change (less than 0.5 cm^{-1}) with increasing the laser power. A careful change of the laser power shows that the integrated peak intensity exhibits a sudden rise at a threshold of 0.6 mW. Figure 3 shows another example with a Raman peak around $\sim$186 cm^{-1}. In this case, though we find the frequency shift at saturated power, the integrated peak intensity exhibits a sudden rise at about 0.16 mW which corresponds to

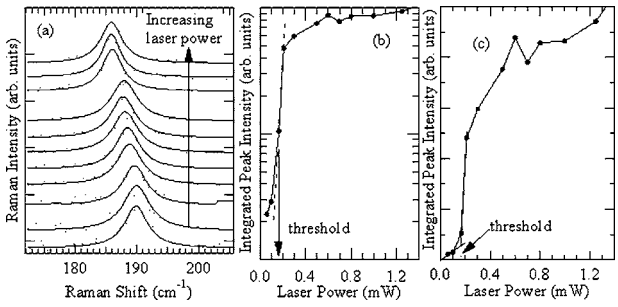

FIG. 3. (a) Raman spectra of a RBM mode at $\sim$186 cm^{-1} under different excitation laser intensities (from bottom: 0.06, 0.1, 0.17, 0.21, 0.3, 0.5, 0.6, 0.7, 0.8, 1, and 1.25 mW). [(b) and (c)] Plot of the integrated peak intensity as a function of laser intensity in logarithm-linear and linear-linear scales, respectively. The threshold of laser intensity for stimulated Raman scattering was 0.16 mW.

0.16 μW when considering the volume of an individual SWNT. This threshold power is below that where the frequency begins to change and thus the shift of the frequency and the existence of the threshold are phenomena independent of each other. The features of the existence of a threshold and a fast increase of the intensity above the threshold power are definite evidences for SRS. We tried to assign (n,m) values for these RBM frequency and laser energy (1.96 eV) by referencing the RBM frequency observed for an isolated SWNT on SiO_2 surfaces, but failed within the accuracy of 10 cm^{-1} and 0.1 eV, respectively, for RBM frequency and excitation laser energy. The reasons for the discrepancy are the different dielectric constant around a SWNT and the temperature of a SWNT. Nevertheless, the observed RBM frequency and 1.96 eV laser energy correspond to the resonance conditions for a metallic SWNT and thus we expect a higher thermal transport property by free electrons in a metallic SWNT than that in a semiconducting nanotube.

SRS is caused by the nonlinear interaction between the lattice vibrations (phonons, frequency ω_P) and the electric fields of light (photons).[5] An electric field can cause the formation of a dipole via polarization of the charge distribution in the material. If the induced dipole is simultaneously modulated by a normal mode of vibration of the material lattice, the mode is said to be Raman active. The dipole can radiate and is the origin of spontaneous Raman scattering, whose intensity is a linear function of the intensity of the incident laser light. On the other hand, SRS is a third-order nonlinear optical process in which the lattice vibration is excited by electric fields. In this case, the force exerted on the vibrating lattice by the electric field is proportional to E^2, where E is the amplitude of the electric field. This means that there must be two photons driving the interaction with the lattice. If the two photons are at different frequencies, the lattice will experience a force at the beat frequency of the two photons. If the frequencies of the two photons are chosen such that their beat frequency equals that of the phonon, strong amplification of the three waves (two electric fields and one lattice vibration) can occur due to the phase-matching interaction, resulting in the stimulated scattering condition. Thus in the present SRS, the two electric fields come from the incident laser light (frequency ω_L) and the Stokes-Raman light (frequency $\omega_S=\omega_L-\omega_P$). The beat frequency of ω_L and ω_S is nothing but ω_P. This is the nonlinear amplification mechanism of the phonon, which eventually leads to the occurrence of SRS. As a nonlinear process, SRS usually occurs at high excitation intensities. The phonon amplification under laser excitation in a SWNT has been demonstrated theoretically,[6] in which the incident direction and polarization of the laser were assumed to be the same as those used in our study. The frequency of the incident light was assumed to be the same as that of the optical phonon, which is also consistent with our experiment because the nonlinear interaction between the incident laser and the Raman light can generate the light having the same frequency as the lattice vibrations (phonons).

Using the exponential law, $I_{\text{out}} \propto \exp(g \cdot I_{\text{in}} \cdot L)$, for the output intensity,[7] the SRS gain g, estimated from the slope of the dashed lines in the figure, was estimated to be $\sim 1 \times 10^9$ and $\sim 6 \times 10^9$ cm/GW for Figs. 2 and 3 respectively. Here I_{in} is the density of the incident laser light. L is the interaction length of the Raman media, which is taken as the tube length (~ 1 μm).[8] The gain value is more than five or-

ders higher than that reported for GaInAs/AlInAs quantum cascade Raman lasers ($\sim 10^4$ cm/GW),[9] and more than eight orders higher than that reported for bulk materials such as Si Raman lasers[10] and other Raman crystals (~ 10 cm/GW),[7] revealing the very high potential of SWNTs as nonlinear optical materials and devices. The Raman gain is written by[7] $g=(4\pi^2\omega_S N/\mu_L\mu_S c^2 m\omega_R\Gamma)\cdot(\partial\alpha/\partial q)^2$, where ω_S and ω_R are the frequencies of Raman lines and lattice vibrations, respectively. μ_L and μ_S are refractive indices of the Raman media for the laser and Raman lines, respectively. N is the number of Raman active atoms. c is the light velocity and m is the reduced mass for the oscillating molecule. Γ is the linewidth of the Raman line (half-width at half-maximum). $\partial\alpha/\partial q$ is the normal-mode derivative of the atomic polarizability tensor caused by the interaction with electric fields, and $(\partial\alpha/\partial q)^2$ is proportional to the imaginary part of χ_3, the third-order nonlinear optical susceptibility. Therefore, the Raman gain is also written as $g\propto \mathrm{Im}(\chi_3)$. It is thus clear that a large Raman gain is expected for the material with a large $\mathrm{Im}(\chi_3)$ value. The values of $\mathrm{Im}(\chi_3)$ of conventional semiconductors such as GaAs and Si are in the order of 10^{-10} esu.[11] For SWNTs, however, $\mathrm{Im}(\chi_3)$ is as high as 10^{-6} esu at resonant wavelength, which is four orders higher.[3] This will unambiguously enhance the Raman gain of SWNTs as observed here. Because of the one-dimensional van Hove singularity of density of states in SWNTs, the Raman signal is strongest when the photon energy of the laser light is exactly equal to the energy differences between the discrete levels of valence and conduction bands of a SWNT, i.e., at a resonant excitation.[1] Therefore, the resonant condition is automatically achieved in this study. Moreover, due to the one-dimensional quantum wire structure, the movement of electrons is strictly restricted along the tube axis. Thus, all of the light-generated electrons are expected to be involved in the electron-phonon interaction and results in significant amplification of phonons.[6] Therefore, the efficiency of electron-phonon interaction in a SWNT is much higher than that in a bulk crystal because, in the latter, the light-generated electrons can propagate in all possible directions. Due to both the resonant excitation and the high interaction efficiency, very large Raman gain and low threshold can be obtained in a SWNT. The threshold laser power to achieve SRS in a SWNT was a few orders of magnitude lower compared with bulk Si-based optical pumped cw Raman lasers (~ 100 mW).[10] Such Si Raman lasers were under nonresonant excitation and were realized by using a waveguide structure, a long interaction length (as long as 4.8 cm), a *p-i-n* structure, and a Fabry-Pérot cavity. In the present work, although a natural nano cavity effect might have occurred, such complicated treatments are not intentionally necessary. Therefore, better Si Raman lasers may be expected by adopting both Si nanowires and resonant excitations. We believe that, by using direct band gap materials, their high-quality nanowire structures with narrow Raman linewidths and resonant excitations, Raman lasers having large gains and low thresholds can be realized.

The observation of the SRS with an extremely large gain and low threshold indicates the very high potential of application of SWNTs as nonlinear optical materials and devices. For example, a wide range, tuneable cw Raman laser can be obtained under the excitation of a commonly used cw He–Ne laser via various SWNTs with different Raman frequencies or different tube diameters. Raman spectroscopy on SWNT has been studied widely.[12] However, no SRS has been reported. The suspending structure used in this study is believed to facilitate the observation of SRS, because the SWNT was freestanding and not suffering from any kind of external disturbances (for example, tube-tube and tube-substrate interactions). These effects should cause random scattering of phonons and electrons propagating in the tube, which will greatly reduce the possibility of achievement of phase matching between lattice vibration (phonon) and light field (or electron). As a result, the possibility of achieving SRS should be substantially suppressed.

The peak position and linewidth also exhibited some dependence on the laser power. In Fig. 2, almost no peak shift (~ 0.5 cm^{-1}) was observed when the laser power was raised to 2.0 mW, while in Fig. 3, the shift was about 4 cm^{-1} up to 1.4 mW. The shift is presently interpreted as the result of a thermal effect. In Fig. 2, the linewidth changed from 1.8 to 2.2 cm^{-1} with increasing the laser power. The width is smaller than the natural linewidth (3 cm^{-1}) reported for SWNTs,[13] revealing that the SWNT is of high quality. On the other hand, in Fig. 3, the linewidth was relatively larger, from 4 to 6 cm^{-1}. Therefore, it is likely that for a narrow Raman line, its peak position is stable; while for a broad one, the peak position is unstable when changing the laser power. These phenomena may be correlated with the tube quality and thermal conductivity: high-quality tubes, indicated by narrow Raman widths, are characterized by high thermal conductivity and then weak thermal effect. On the contrary, low-quality tubes, indicated by broad Raman widths, are characterized by low thermal conductivity and then strong thermal effect. Another possibility is that, for broad Raman lines, there were originally more than one tube being probed. With increasing the laser power, especially when it is over the threshold, the resonant condition changed and the signal from a different tube becomes resonant. This situation will be confirmed by using a tuneable laser system.

[1] S. M. Bachilo, M. S. Strano, C. Kittrell, R. H. Hauge, R. E. Smalley, and R. B. Weisman, Science **298**, 2361 (2002).
[2] J. A. Misewich, R. Martel, P. Avouris, J. C. Tsang, S. Heinze, and J. Tersoff, Science **300**, 783 (2003).
[3] A. Maeda, S. Matsumoto, H. Kishida, T. Takenobu, Y. Iwasa, M. Shiraishi, M. Ata, and H. Okamoto, Phys. Rev. Lett. **94**, 047404 (2005).
[4] B. P. Zhang, S. Shimazaki, M. Suzuki, T. Shiokawa, Y. Homma, and K. Ishibashi, Microelectron. Eng. **87**, 1736 (2006).
[5] J. Reintjes and M. Bashkansky, in *Handbook of Optics*, 2nd ed., edited by M. Bass (McGraw-Hill, New York, 2001), Vol. IV, chap. 18.
[6] F. Peng, Europhys. Lett. **73**, 116 (2006).
[7] H. M. Pask, Prog. Quantum Electron. **27**, 3 (2003).
[8] Due to the one-dimensional quantum wire shape of a SWNT, the movement of electrons is strictly restricted along the tube axis. Therefore, the interaction length is in the same order as that of the tube length.
[9] M. Troccoli, A. Belyanin, F. Capasso, E. Cubukcu, S. L. Sivco, and A. Y. Cho, Nature (London) **433**, 845 (2005).
[10] H. Rong, R. Jones, A. Liu, O. Cohen, D. Hak, A. Fang, and M. Paniccia, Nature (London) **433**, 725 (2005).
[11] D. J. Moss, E. Ghahramani, and J. E. Sipe, Phys. Status Solidi B **164**, 587 (1991).
[12] M. S. Dresselhaus, G. Dresselhaus, R. Saito, and A. Jorio, Phys. Rep. **409**, 47 (2005).
[13] A. Jorio, M. A. Pimenta, A. G. Souza Filho, R. Saito, G. Dresselhaus, and M. S. Dresselhaus, New J. Phys. **5**, 139 (2003).